European Journal of Cancer (2013) 49, 616–624

Available at www.sciencedirect.com

SciVerse ScienceDirect

journal homepage: www.ejcancer.info

Ultrasmall superparamagnetic particles of iron oxide allow for the detection of metastases in normal sized pelvic lymph nodes of patients with bladder and/or prostate cancer ☆

Maria Triantafyllou [a], Urs E. Studer [b], Frédéric D. Birkhäuser [b], Achim Fleischmann [c], Lauren J. Bains [a], Giuseppe Petralia [a], Andreas Christe [a], Johannes M. Froehlich [a], Harriet C. Thoeny [a,*]

[a] *Department of Radiology, Neuroradiology and Nuclear Medicine, Institute for Diagnostic, Interventional, and Pediatric Radiology, Inselspital University Hospital Bern, Switzerland*
[b] *Department of Urology, Inselspital University Hospital Bern, Switzerland*
[c] *Department of Pathology, Inselspital University Hospital Bern, Switzerland*

Available online 18 October 2012

KEYWORDS
Bladder cancer
Prostate cancer
Lymph nodes
Metastases
MRI
USPIO
Surgery
Histopathology

Abstract ***Aim:*** Lymph node metastases influence prognosis and outcome in patients with bladder and prostate cancer. Cross sectional imaging criteria are limited in detecting metastases in normal sized lymph nodes. This prospective study assessed the diagnostic accuracy of ultrasmall superparamagnetic particles of iron oxide (USPIO)-enhanced magnetic resonance imaging (MRI) for the detection of metastases in normal sized lymph nodes using extended pelvic lymph node dissection (ePLND) and histopathology as the reference standard.
Methods: Seventy-five patients (bladder cancer, $n = 19$, prostate cancer $n = 48$, both, $n = 8$) were examined using 3T MR before and after USPIO-administration. A preoperative reading with two readers in consensus and a second postoperative reading with three independent blinded readers were performed. Results were correlated with histopathology and diagnostic accuracies were calculated for all readings.
Results: A total of 2993 lymph nodes were examined histopathologically. Fifty-four metastatic nodes were found in 20/75 patients (26.7%). The first reading had a sensitivity of 55.0%, specificity of 85.5%, positive predictive value (PPV) of 57.9%, negative predictive value (NPV) of 83.9%, and diagnostic accuracy (DA) of 77.3% on a per patient level. The second

☆ The protocol of this prospective study was conducted in accordance with the Declaration of Helsinki and Good Clinical Practice guidelines and approved by the regional ethics committee, and registered on www.clinicaltrial.gov under NCT00622973. Written informed consent was obtained from all patients prior to inclusion.

* *Corresponding author:* Address: Department of Radiology, Neuroradiology and Nuclear Medicine, Institute for Diagnostic, Interventional, and Pediatric Radiology, Inselspital University Hospital Bern, Freiburgstrasse 10, Bern 3010, Switzerland. Tel.: +41 31 632 2939; fax: +41 31 632 4874.
E-mail address: harriet.thoeny@insel.ch (H.C. Thoeny).

http://dx.doi.org/10.1016/j.ejca.2012.09.034

reading had a mean sensitivity of 58.3%, specificity of 83.0%, PPV of 58.0%, NPV of 84.4% and DA of 76.4% on a per patient level. The majority of missed metastases were smaller than 5 mm in short axis diameter.

Conclusions: USPIO-enhanced MRI in bladder and prostate cancer patients allows detection of metastases in normal sized lymph nodes and might guide the surgeon to remove suspicious lymph nodes not included in standard PLND.

1. Introduction

Metastatic involvement of lymph nodes in patients with bladder and/or prostate cancer has a strong impact on treatment decisions and patient prognosis.[1–5] Although size and morphology are used to evaluate lymph node involvement using conventional cross sectional imaging, there is a limited ability to detect metastases in normal sized lymph nodes using these criteria. Therefore, an extended template pelvic lymph node dissection (ePLND) is preferred by many urologists, even when no lymph node metastases are detectable on computerised tomography (CT) or magnetic resonance imaging (MRI) (N0 staging).[6–8] In fact, occult lymph node metastases are found in template lymphadenectomy in up to 25% of patients staged as N0.[5,7,9,10] It is also known that lymph node metastases in patients with bladder and/or prostate cancer do not necessarily follow a predefined pathway of spread,[11] and that even when PLND is extended to the mid-upper third of the common iliac vessels, only about 90% of the primary lymphatic landing sites are removed.[6–8,12] Thus, ePLND remains the gold standard for the detection of lymph node metastases in patients with urogenital cancers.[13–16] Although restricted lymph node dissection and targeted local treatments are desirable, these can only be performed if accurate preoperative lymph node staging is possible.

In order to improve detection of lymph node metastases, the use of lymphotropic ultrasmall superparamagnetic particles of iron oxide (USPIO) has been investigated in several urogenital malignancies.[17–26] Promising results with apparent diagnostic accuracies up to 97.3% have been published; however, none of the previous studies were based on ePLND. Therefore, the accuracy of the published negative predictive values is limited. Moreover, the majority of the published studies included patients with enlarged lymph nodes, and few authors commented on the detection of metastases in normal sized lymph nodes after the administration of USPIO.[18,26]

Thus, the aim of our study was to prospectively assess the diagnostic accuracy of USPIO-enhanced MRI for the detection of lymph node metastases in bladder and/or prostate cancer patients with N0 staging based on conventional MR/CT imaging using meticulous ePLND and histopathology as the reference standard.

2. Methods

2.1. Patients

Between May 2008 and March 2010, 256 patients with histologically proven invasive bladder and/or prostate cancer were scheduled for radical cysto-/prostatectomy and ePLND (Fig. 1). Patients with prior chemotherapy or radiotherapy in the pelvic area, enlarged pelvic lymph nodes on previous CT/MRI (threshold of 10 mm in short axis diameter for bladder and 8 mm for prostate cancer), positive bone scintigraphy, hemochromatosis, gadolinium administration 48 h prior to the examination, known iron or dextrane allergy or MR contraindications were excluded. Finally, 84 of these patients were initially eligible for study inclusion.

Nine of these 84 patients were secondarily excluded due to the detection of bone metastases on study MRI contraindicating surgery ($n = 1$), detection of enlarged lymph nodes on the MR images ($n = 2$), unacceptable image quality ($n = 1$), inductive chemotherapy following positive imaging results ($n = 2$), allergic reaction to USPIO ($n = 1$), refusal of surgery ($n = 1$) or cancellation of surgery due to poor performance status ($n = 1$). A total of 75 patients qualified for final image analysis and represented the study cohort (Table 1).

2.2. Imaging

All patients were examined on a 3T MR unit (Trio, Siemens Medical, Erlangen, Germany). Two identical pelvic MRI exams were performed before and 24–36 h after intravenous administration of 2.6 mg iron/kg body weight of USPIO (Ferumoxtran-10, Sinerem®; Guerbet, Roissy, France). One milligram of Glucagon (GlucaGen, Novo Nordisk, Switzerland) was administrated intravenously at the beginning of each MR exam. Adverse events such as urticaria ($n = 2$), hot flash, hypertension and headache ($n = 2$), swelling of neck and nose ($n = 1$) and diarrhoea ($n = 2$) occurred in seven (11%) patients. In an eighth patient USPIO injection was stopped when dyspnoea and hypertension occurred after injection of 2 ml USPIO solution. Symptoms were self-limiting in all cases.

A 3D T1-weighted (T1w) sequence with 0.8 mm^3 reconstructed isotropic voxels, and an iron-sensitive

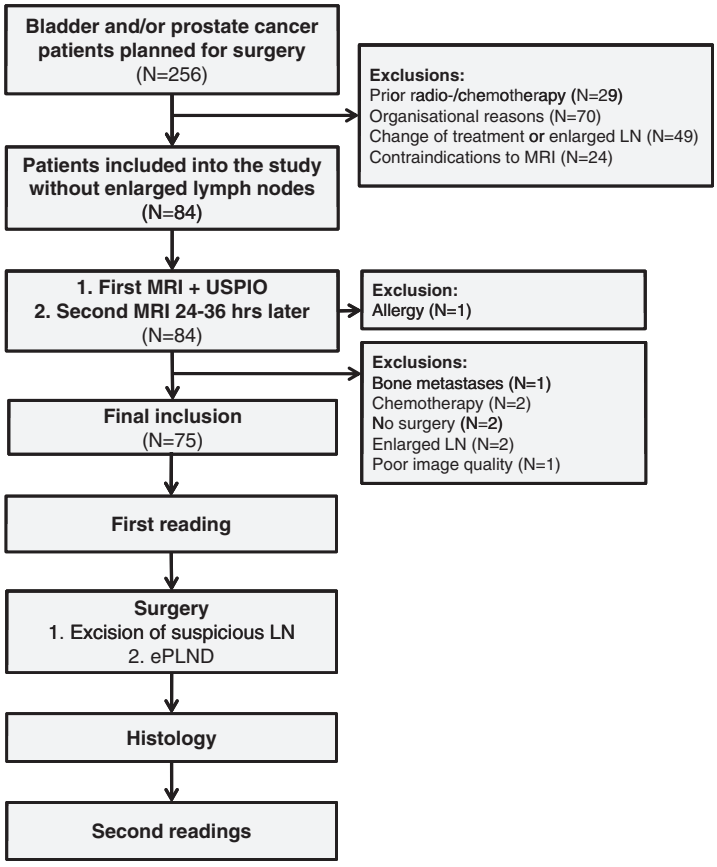

Fig. 1. Trial progress flowchart. MRI, magnetic resonance imaging; ePLND, extended pelvic lymph node dissection; USPIO, ultrasmall superparamagnetic particles of iron oxide; LN, lymph nodes.

Table 1
Patient and tumour characteristics including demographics and postoperative tumour and lymph node staging.

Patient characteristics	Median	Range
Age (years)	64	43–82
Days between MR and surgery	8	0–33
Gleason score	7	5–9
Number of LN sampled per patient	39	17–68
Patient characteristics		Participants
Gender		
Male		66
Female		9
Tumour type		
Bladder cancer		19
Prostate cancer		48
Bladder and prostate cancer		8
Bladder cancer staging		
pT1G3		2
pT2G any		11
pT3G any		12
pT4G any		2
Prostate cancer staging		
pT1		2
pT2		31
pT3		18
pT4		5

Abbreviations: MR = magnetic resonance; LN = lymph nodes.

3D T2-weighted (T2w) sequence with 1.0 mm^3 isotropic voxels were performed in the coronal plane through the entire pelvis. In addition, a 3D T1w-VIBE sequence was obtained during the second MRI exam to facilitate the exact anatomical localisation of the lymph nodes in relation to the blood vessels. Additional diffusion-weighted MRI sequences were performed but not evaluated in the present study.

2.3. Radiological evaluation

Radiological evaluation was performed on a picture archiving and communication system (PACS) workstation (PACS R11.4.1, 2009; Philips, Best, Netherlands; Sectra, Linköping, Sweden). A preoperative reading was performed by two readers in consensus out of a pool of four (M.T., H.C.T., G.P., J.M.F. with 3, 12, 5 and 8 years of experience in body MRI, respectively). After finishing the patient accrual a second postoperative reading was performed by three readers independently (G.P., A.C. and M.T.), blinded to histopathology results and clinical information. Reader A (G.P.) was a radiologist with six years of MRI experience and one year of experience in USPIO-enhanced MRI, Reader B (A.C.) had five years of experience in MRI and a short training

in reading USPIO-enhanced MRI. Reader C (M.T.) was a radiologist with five years of MRI experience and two years of USPIO-enhanced MRI experience.

2.4. Image interpretation

A node-by-node analysis was performed on axially reconstructed (2 mm slices) T2w-sequences by comparing images before and after USPIO-administration. Lymph nodes were considered benign when a signal intensity loss of >15% on the post-USPIO images was observed,[27] and malignant when signal intensity was largely maintained in areas which did not correspond to hilar fat (Fig. 2). Localisation of suspicious nodes was indicated on an anatomical landmark chart dividing the pelvis into ten regions (Fig. 3). Imaging results were reviewed with the responsible surgeon after the first reading to ensure removal of suspicious lymph nodes.

The entire time of evaluation was noted for all readings.

2.5. Surgery

Prior to PLND, lymph nodes indicated on the landmark chart were resected, labelled and sent for separate histopathological examination. An ePLND including the area of the crossing of the ureters and the common iliac vessels was then performed.[6,12] Specimens from ePLND were labelled according to the ten anatomical regions.

2.6. Histopathological evaluation

Resected lymph nodes were fixed overnight in 4% formalin, degreased with acetone, cut into 2–4 mm thick tissue slices and completely embedded in paraffin. One section per paraffin block was taken for histopathological examination. Two experienced pathologists evaluated histopathological findings that could influence the uptake of USPIO in each lymph node, including follicular hyperplasia, sinus histiocytosis, marked fibrosis,

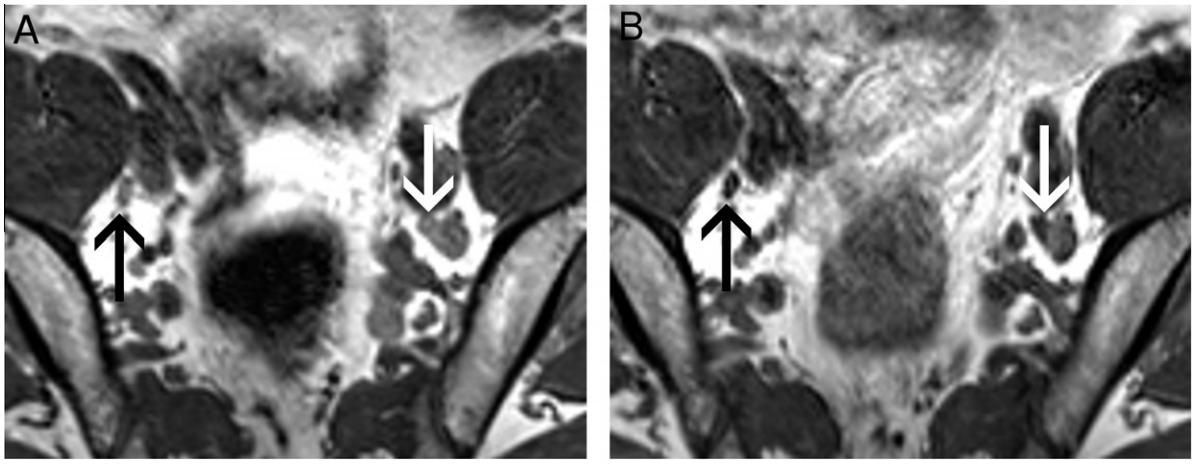

Fig. 2. Typical example of ultrasmall superparamagnetic particles of iron oxide (USPIO) uptake in positive and negative lymph nodes. Axial T2w-reconstructed images before (A) and after (B) the administration of USPIO in a 67-year-old prostate cancer patient. The benign lymph node (black arrow) shows a decrease in signal intensity after the uptake of USPIO; the malignant lymph node (white arrow) shows only partial posterior and medial signal decrease after the administration of USPIO.

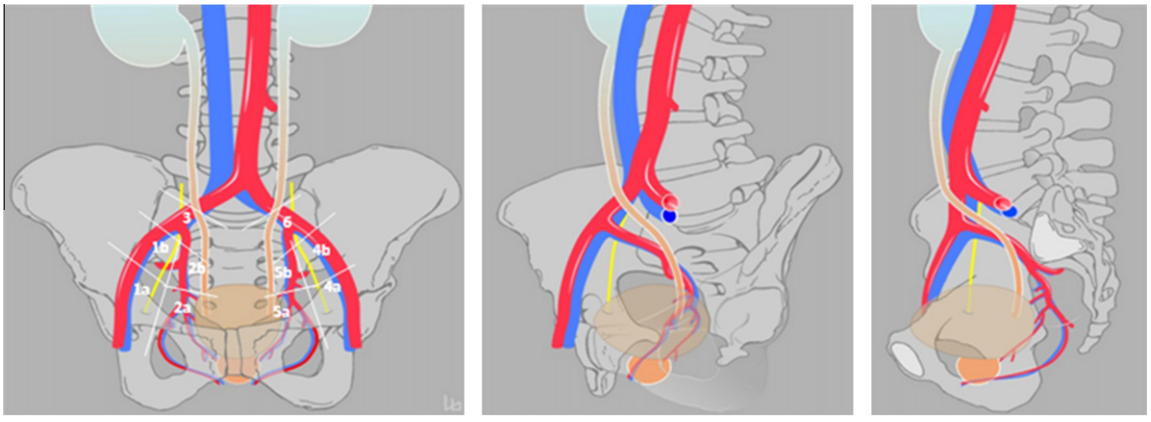

Fig. 3. Anatomic landmark chart divided into 10 regions according to the iliac vessels: common iliac right (3) and left (6), proximal external iliac right (1b) and left (4b), distal external iliac right (1a) and left (4a), proximal internal iliac right (2b) and left (5b), distal internal iliac right (2a) and left (5a).

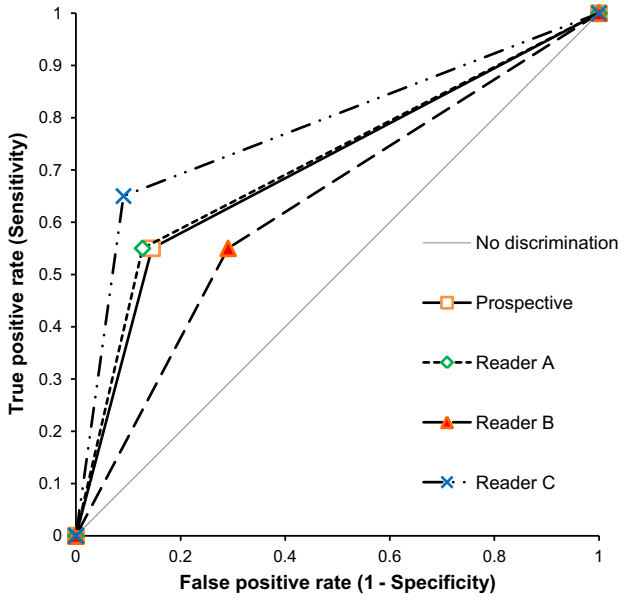

Fig. 4. Receiver operating characteristic (ROC) curves showing the diagnostic performance of the first (prospective) and second (A, B, C) readings on a per patient level.

marked fatty involution and neoplastic tissue. Sizes of positive lymph nodes and metastases were measured in two planes and localisations on the anatomic landmark chart were recorded.

2.7. Statistics

All included patients were staged N0. Statistical performance measures (i.e. sensitivity, specificity, positive predictive value (PPV), negative predictive value (NPV) and accuracy) of the USPIO readings as compared to histopathological findings were calculated both on a per patient and per pelvic side level for both readings.

Table 2
Patients with unilateral and bilateral pelvic lymph node metastases.

Number of lymph node metastases per patient	Patients with unilateral pelvic involvement	Patients with bilateral pelvic involvement
1	8	0
2	2	3
3	3	1
4	0	2
>4	0	1

Statistical analyses were performed using Microsoft Excel with the Analyse-it plugin (Release 2.22/2010; Analyse-it Software Ltd., Leeds, United Kingdom; Microsoft, Redmont, USA). Receiver operating characteristic (ROC) curve analyses were performed using histopathological results as gold standard (Fig. 4).

Interobserver agreement between the three blinded readers in the second reading was assessed on a per patient level using Fleiss's kappa statistic and Randolph's free-marginal multirater kappa statistic for all four readings, where a kappa of 1.0 indicates perfect agreement.[28,29]

3. Results

3.1. Histopathological evaluation

A total of 2993 lymph nodes were identified in 75 patients. Fifty-four metastases (1.8% of resected lymph nodes) were found in 20/75 (26.7%) patients. Thirteen patients presented with unilateral metastases (Table 2). Histopathology reported four metastatic lymph nodes having a short axis diameter >10 mm. Most of the malignant lymph nodes had a short axis diameter ⩽5 mm (41/54) (Fig. 5). The majority of the metastases themselves had a short axis diameter ⩽5 mm (50/54), and 43/54 were ⩽3 mm in short axis diameter (Table 3).

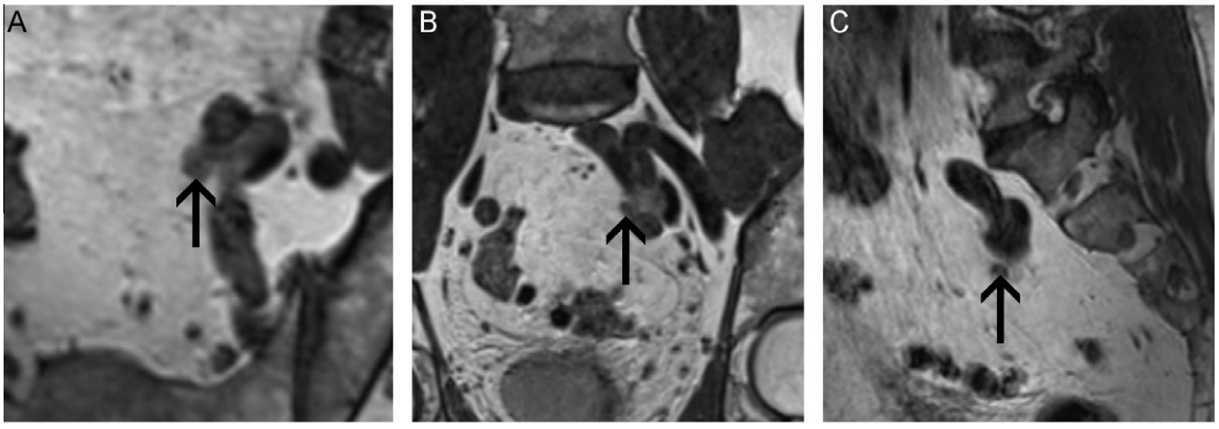

Fig. 5. Example of a correctly diagnosed positive lymph node metastasis localised between the left proximal internal and external iliac artery (black arrow) shown in axial reconstructed T2w-images after ultrasmall superparamagnetic particles of iron oxide (USPIO) administration (A), coronally acquired T2w-images (B) and parasagittal reconstructions (C) in a 60-year-old patient with bladder and prostate cancer. This lymph node did not show USPIO uptake. Such a metastasis may have easily been missed in extended pelvic lymph node dissection (ePLND) in the absence of imaging results.

Table 3
Number of lymph node metastases classed by size of lymph nodes and metastases as determined by histopathology. Note that the largest lymph nodes and metastases (*) were not visible on magnetic resonance imaging (MRI) retrospectively, which may be related to the differing planes of MR imaging and histopathological sections.

Size (mm)	Lymph nodes (*n*)	Metastases (*n*)	
	Short axis	Short axis	Long axis
⩽1	4	20	16
1.1–3.0	12	23	11
3.1–5.0	25	7	18
5.1–8.0	6	3	3
8.1–10.0	3	0	1
>10	4*	1*	5*

Table 4
Diagnostic performance per patient ($n = 75$).

Per patient: statistical performance measures	First reading	Second reading			
		Reader A	Reader B	Reader C	Average
True positive	11	11	11	13	11.7
False positive	8	7	16	5	9.3
False negative	9	9	9	7	8.3
True negative	47	48	39	50	45.7
Sensitivity (%)	55.0	55.0	55.0	65.0	58.3
Specificity (%)	85.5	87.3	70.9	90.9	83.0
Positive predictive value (%)	57.9	61.1	40.7	72.2	58.0
Negative predictive value (%)	83.9	84.2	81.3	87.7	84.4
Diagnostic accuracy (%)	77.3	78.7	66.7	84.0	76.4

Table 5
Diagnostic performance per pelvic side ($n = 150$).

Per pelvic side: statistical performance measures	First reading	Second reading			
		Reader A	Reader B	Reader C	Average
True positive	12	11	11	17	13
False positive	13	12	24	7	14.3
False negative	14	15	15	9	13
True negative	111	112	100	117	109.7
Sensitivity (%)	46.2	42.3	42.3	65.4	50.0
Specificity (%)	89.5	90.3	80.6	94.4	88.4
Positive predictive value (%)	48.0	47.8	31.4	70.8	50.0
Negative predictive value (%)	88.8	88.2	87.0	92.9	89.4
Diagnostic accuracy (%)	82.0	82.0	74.0	89.3	81.8

Results are similar for long axis diameter measurements (Table 3).

3.2. Diagnostic performance on a per patient level

In the first reading a sensitivity of 55.0%, specificity of 85.5%, PPV of 57.9%, NPV of 83.9% and diagnostic accuracy (DA) of 77.3% were observed (Table 4), and 11/20 patients were correctly diagnosed as positive. In the second reading, combining the results of all three independent readers gave a mean sensitivity of 58.3%, mean specificity of 83.0%, mean PPV of 58.0%, mean NPV of 84.4% and mean DA of 76.4% (Table 4). Readers A, B and C correctly detected metastases in 11/20, 11/20 and 13/20 patients, respectively, and gave false negative readings in 9/20, 9/20 and 7/20 patients (Table 4).

3.3. Diagnostic performance on a per pelvic side level

On a per pelvic side level ($n = 150$) a sensitivity of 46.2%, specificity of 89.5%, PPV of 48.0%, NPV of 88.8% and DA of 82.0% were reported in the first reading. Metastases were correctly detected in 12/26 positive sides. In the second reading a mean sensitivity of 50.0%, specificity of 88.4%, PPV of 50.0%, NPV of 89.4% and DA of 81.8% were observed for readers A, B and C, respectively (Table 5).

3.4. Detection of small metastases

Apart from one metastasis with a short axis diameter of >5 mm which was missed by one reader, all other missed metastases were ⩽5 mm, and most were ⩽3 mm in short axis diameter. A total of 17 metastases with a short axis diameter ⩽5 mm were correctly detected by the most experienced reader. Some anatomical regions were particularly difficult to evaluate for small (⩽5 mm) metastases, including the perivesical and periprostatic area and lymph nodes along the common iliac vessels. A periprostatic metastasis of 0.5×0.2 mm and a metastasis in the perivesical fat of 0.28×0.28 mm were missed in all four readings. Small metastases close to the common iliac vessels also remained undetected in all four readings (Table 5 and Fig. 6).

False positive results could be attributed in single cases to marked fibrosis or lipomatosis (Fig. 7).

3.5. Interobserver agreement of second reading

Interrater agreement for the four readings yielded a Fleiss' kappa of 0.77 and a Randolph's multirater kappa of 0.54, indicating a moderate interrater agreement.[28,29]

3.6. Time of evaluation for the MRI readings

The time of evaluation for the preoperative MRI reading ranged from 10 to 93 min with a median value

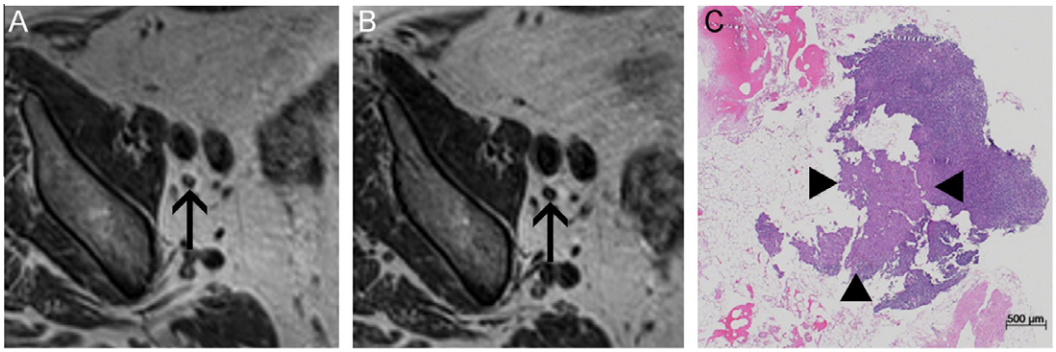

Fig. 6. Example of a false negative lymph node (black arrow). Axial reconstructed T2w-images before (A) and after (B) the administration of ultrasmall superparamagnetic particles of iron oxide (USPIO) in a 68-year-old patient with prostate cancer. The lymph node shows a signal intensity decrease of 55%. Histopathology showed a metastasis of 2.3 × 0.8 mm (short arrows, C) in a lymph node by the left common iliac artery. No other metastatic lymph nodes were identified in this patient.

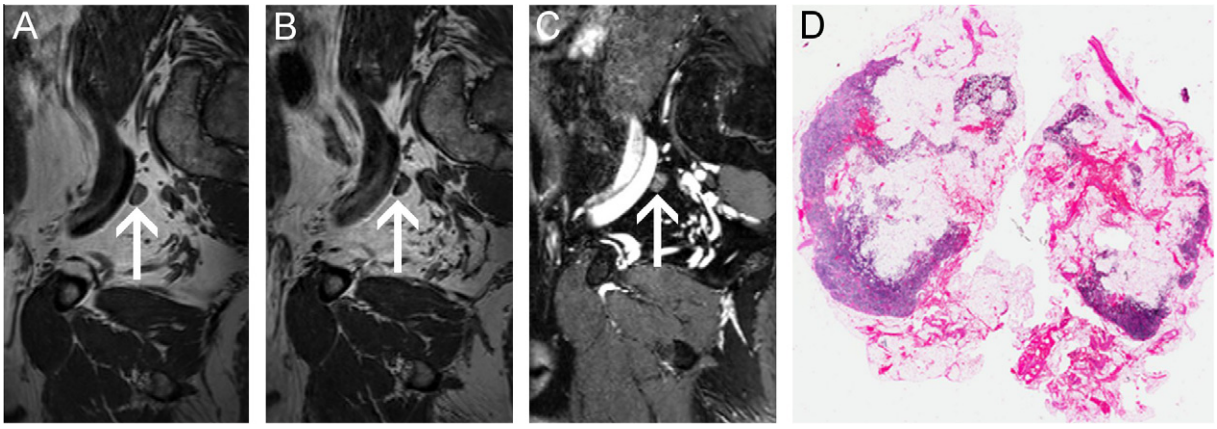

Fig. 7. Example of a false positive lymph node (white arrow). T2w-parasagittal reconstructed images are shown before (A) and after (B) the administration of ultrasmall superparamagnetic particles of iron oxide (USPIO) in a 66-year-old patient with bladder and prostate cancer. The lymph node did not show any significant drop of signal intensity after the administration of USPIO. Parasagittal reconstructed VIBE images show the localisation of the suspicious lymph node in relation to the vessels (C). Histopathology shows the presence of extensive fatty tissue replacing parts of the lymph node (lipomatosis) (D).

of 45 min per patient and for the second reading from 10 to 47 min with a median of 32 min per patient.

4. Discussion

Our results indicate that USPIO-enhanced MRI enables detection of lymph node metastases in normal sized lymph nodes in bladder and prostate cancer patients staged as metastasis free (N0) based on conventional cross sectional imaging methods. These results are in agreement with previously published data which show that USPIO-enhanced MRI improves pelvic lymph node staging in patients with urogenital malignancies.[18–20,26] Despite the limited spatial resolution of MRI, we were even able to detect lymph node metastases smaller than 5 mm. Using ePLND as reference standard, the results of the present study provide an accurate portrayal of the diagnostic potential of USPIO-enhanced MRI. Due to the still substantial number of false negative readings, USPIO-enhanced MRI cannot replace ePLND. However, we have demonstrated that USPIO-enhanced MRI provides valuable additional information which could guide the surgeon to extend the region of standard PLND.

The diagnostic accuracies reported here are relatively low compared to previous literature. This may be partially attributed to the exclusion of patients with enlarged lymph nodes from this study. In a study including bladder cancer patients, those authors found 38/50 positive lymph nodes larger than 10 mm.[26] In another study including prostate cancer patients, 38/63 positive nodes fulfilled the morphological imaging criteria of malignancy.[18] The inclusion of lymph nodes with suspicious morphology partially explains the higher sensitivity and positive predictive values reported in these studies. Although our final histopathological results showed four metastatic nodes having a short axis diameter >10 mm, these nodes were not detectable on retrospective review of the MR images. This may be related to the differing planes of MR imaging and histopathological sectioning.

Another strength of the present study is the high number of lymph nodes that were resected (mean of

39 per patient) explaining the lower diagnostic accuracy compared to previous studies.[6,12] Additionally, a meticulous histopathological analysis of each lymph node lead to the detection of micrometastases as small as 0.1×0.2 mm. This is significant because the likelihood that micrometastases will be found increases with the number of normal sized nodes removed[7] and the sensitivity of our diagnostic assays was correspondingly lower. In a study of prostate cancer patients, 334 lymph nodes were resected or biopsied in 80 patients which corresponds to an average of four nodes per patient, suggesting that primarily enlarged nodes and nodes suspicious for metastases on USPIO-enhanced MRI were analysed.[18] This results in an overestimation of the diagnostic accuracy since the number of missed metastases in normal sized LNs is unknown in the absence of histopathological results.

As in previously published literature,[18,19] false positive results were often found in conjunction with conditions influencing the normal architecture and function of lymph nodes such as fibrosis, sinus histiocytosis, lipomatosis or focal fatty involution which may lead to heterogeneous uptake of USPIO. However, from a clinical point of view, false positive findings are of lesser importance than false negatives since the removal of false positive nodes does not harm the patient, while missing metastatic nodes can negatively impact patient prognosis. Thus, the relatively high negative predictive value on a per patient level in our study demonstrates the potentially useful role of USPIO-enhanced MRI in patient management.

In contrast to previous studies, our investigation was performed on a 3T MR unit providing improved image quality relative to 1.5T MR. This allowed for high image resolution with reconstructed isotropic voxel sizes as small as 0.8 mm^3, which was crucial to the detection of small metastases. However, the majority of metastases with a short axis diameter $\leqslant$3 mm were still missed.

Our study has several limitations. Firstly, node-by-node correlations of MRI with histopathology could not be performed. However, the localisation of lymph nodes in ten well defined anatomical regions allowed nodes seen on MRI to be targeted surgically. Secondly, we refrained from individual analysis of the ten sectors as initially planned, because the boundaries of surgical resection were ill defined and varied depending on the individual surgeon. Therefore, we performed our analysis per pelvic side and per patient. Thirdly, although ePLND was performed with a high number of lymph nodes resected per patient, it is possible that single lymph nodes were missed.

Finally, it must be mentioned that USPIO is not currently approved by health authorities for lymph node detection, despite several attempts and a large number of clinical studies. In anticipation of the development of further USPIO-derivatives, we believe that the present study is important in providing insight into the diagnostic work-up of lymph node metastases and in setting realistic and clinically relevant imaging goals for future studies.

The present data show that the use of USPIO-enhanced MRI in patients with bladder and/or prostate cancer staged as N0 on conventional cross sectional imaging enables the accurate detection of metastases with a short axis diameter of 5 mm and larger. Due to the number of missed metastases smaller than 3 mm, lymph node dissection restricted to suspicious nodes cannot be recommended. However, USPIO-enhanced MRI has the potential to improve treatment and patient outcomes by guiding the removal of additional suspicious nodes in pelvic regions not typically included in standard PLND.

Role of the funding source

The trial was supported by the Swiss National Science Foundation for Research (SNF) 320000-113512, CARIGEST SA, Geneva, representing an anonymous donor, and the Majores Foundation.

The contrast agent Sinerem® was provided free of charge from Guerbet, Roissy CdG, France.

Conflict of interest statement

J.M.F. is a consultant of Guerbet Contrast Media Company, which provided the USPIO contrast agent used in the present study. All other authors declared no conflicts of interest.

Acknowledgements

We thank Frederik De Keyzer, MSc (University Hospitals of Leuven, Belgium) for statistical analysis and support for data presentation. Our special thanks go to Peter Vermathen, PhD and Tobias Binser, PhD for their support during preparation of the study and imaging of patients, and to Michael von Gunten for his great support in the histopathological work-up.

References

1. Walsh PC. Surgery and the reduction of mortality from prostate cancer. *N Engl J Med* 2002;**347**:839–40.
2. Messing EM, Manola J, Sarosdy M, Wilding G, Crawford ED, Trump D. Immediate hormonal therapy compared with observation after radical prostatectomy and pelvic lymphadenectomy in men with node-positive prostate cancer. *N Engl J Med* 1999;**341**: 1781–8.
3. Holmberg L, Bill-Axelson A, Helgesen F, et al. A randomized trial comparing radical prostatectomy with watchful waiting in early prostate cancer. *N Engl J Med* 2002;**347**:781–9.
4. Pagliarulo V, Hawes D, Brands FH, et al. Detection of occult lymph node metastases in locally advanced node-negative prostate cancer. *J Clin Oncol* 2006;**24**:2735–42.

5. Schumacher MC, Burkhard FC, Thalmann GN, Fleischmann A, Studer UE. Good outcome for patients with few lymph node metastases after radical retropubic prostatectomy. *Eur Urol* 2008;**54**:344–52.
6. Burkhard FC, Roth B, Zehnder P, Studer UE. Lymphadenectomy for bladder cancer: indications and controversies. *Urol Clin North Am* 2011;**38**:397–405.
7. Zehnder P, Studer UE, Skinner EC, et al. Super extended versus extended pelvic lymph node dissection in patients undergoing radical cystectomy for bladder cancer: a comparative study. *J Urol* 2011;**186**:1261–8.
8. Briganti A, Rigatti P, Montorsi F. The importance of the extent of pelvic-lymph-node dissection in the diagnosis of lymph-node-metastases in prostate cancer. *Lancet Oncol* 2008;**9**:915–7.
9. Fleischmann A, Thalmann GN, Markwalder R, Studer UE. Extracapsular extension of pelvic lymph node metastases from urothelial carcinoma of the bladder is an independent prognostic factor. *J Clin Oncol* 2005;**23**:2358–65.
10. Bader P, Burkhard FC, Markwalder R, Studer UE. Disease progression and survival of patients with positive lymph nodes after radical prostatectomy. Is there a chance of cure? *J Urol* 2003; **169**:849–54.
11. McLaughlin AP, Saltzstein SL, McCullough DL, Gittes RF. Prostatic carcinoma: incidence and location of unsuspected lymphatic metastases. *J Urol* 1976;**115**:89–94.
12. Roth B, Wissmeyer MP, Zehnder P, et al. A new multimodality technique accurately maps the primary lymphatic landing sites of the bladder. *Eur Urol* 2010;**57**:205–11.
13. Skinner DG. Management of invasive bladder cancer: a meticulous pelvic node dissection can make a difference. *J Urol* 1982;**128**: 34–6.
14. Herr H, Konety B, Stein J, Sternberg CN, Wood Jr DP. Optimizing outcomes at every stage of bladder cancer: do we practice it? *Urol Oncol* 2009;**27**:72–4.
15. Sepherd JH. Revised FIGO staging for gynaecological cancer. *Br J Obstet Gynaecol* 1989;**96**:889–92.
16. Briganti A, Blute ML, Eastham JH, et al. Pelvic lymph node dissection in prostate cancer. *Eur Urol* 2009;**55**:1251–65.
17. Anzai Y, Piccoli CW, Outwater EK, et al. Evaluation of neck and body metastases to nodes with ferumoxtran 10-enhanced MR imaging: phase III safety and efficacy study. *Radiology* 2003;**228**: 777–88.
18. Harisinghani MG, Barentsz J, Hahn PF, et al. Noninvasive detection of clinically occult lymph-node metastases in prostate cancer. *N Engl J Med* 2003;**348**:2491–9.
19. Rockall AG, Sohaib SA, Harisinghani MG, et al. Diagnostic performance of nanoparticle-enhanced magnetic resonance imaging in the diagnosis of lymph node metastases in patients with endometrial and cervical cancer. *J Clin Oncol* 2005;**23**:2813–21.
20. Heesakkers RA, Hövels AM, Jager GJ, et al. MRI with a lymph-node-specific contrast agent as an alternative to CT scan and lymph-node dissection in patients with prostate cancer: a prospective multicohort study. *Lancet Oncol* 2008;**9**:850–6.
21. Hövels AM, Heesakkers RA, Adang EM, Barentsz JO, Jager GJ, Severens JL. Cost-effectiveness of MR lymphography for the detection of lymph node metastases in patients with prostate cancer. *Radiology* 2009;**252**:729–36.
22. Weissleder R, Elizondo G, Wittenberg J, Lee AS, Josephson L, Brady TJ. Ultrasmall superparamagnetic iron oxide: an intravenous contrast agent for assessing lymph nodes with MR imaging. *Radiology* 1990;**175**:494–8.
23. Russell M, Anzai Y. Ultrasmall superparamagnetic iron oxide enhanced MR imaging for lymph node metastases. *Radiography* 2007;**13**:e73–84.
24. Bellin MF, Lebleu L, Meric JB. Evaluation of retroperitoneal and pelvic lymph node metastases with MRI and MR-lymphography. *Abdom Imaging* 2003;**28**:155–63.
25. Heesakkers RA, Fütterer JJ, Hövels AM, et al. Prostate cancer evaluated with ferumoxtran-10-enhanced $T2^*$-weighted MR imaging at 1.5 and 3.0 T: early experience. *Radiology* 2006;**239**:481–7.
26. Deserno WM, Harisinghani MG, Taupitz M, et al. Urinary bladder cancer: preoperative nodal staging with ferumoxtran-10-enhanced MR imaging. *Radiology* 2004;**233**:449–56.
27. Froehlich JM, Triantafyllou M, Fleischmann A, Vermathen P, Thalmann GN, Thoeny HC. Does quantification on USPIO related signal loss allow differentiation of benign and malignant normal sized pelvic lymph nodes? *Contrast Media Mol Imaging* 2012;**7**:346–55.
28. Randolph JJ. Free-marginal multirater kappa: an alternative to Fleiss' fixed-marginal multirater kappa. In: *Joensuu University Learning and Instruction Symposium*, 2005 October 14–15, Joensuu, Finland.
29. Warrens M. Inequalities between multi-rater kappas. *Adv Data Anal Classif* 2010;**4**:271–86.